ResearchGate

See discussions, stats, and author profiles for this publication at: https://www.researchgate.net/publication/231391263

Constrained Nonlinear Estimation for Industrial Process Fouling

ARTICLE *in* INDUSTRIAL & ENGINEERING CHEMISTRY RESEARCH · MAY 2010

Impact Factor: 2.59 · DOI: 10.1021/ie9018116

CITATIONS
14

READS
36

3 AUTHORS, INCLUDING:

John David Hedengren
Brigham Young University - Provo Main Ca…

54 PUBLICATIONS **197** CITATIONS

SEE PROFILE

Available from: John David Hedengren
Retrieved on: 27 January 2016

Constrained Nonlinear Estimation for Industrial Process Fouling

Benjamin J. Spivey,*,† John D. Hedengren,‡ and Thomas F. Edgar†

Department of Chemical Engineering, The University of Texas at Austin, Austin, Texas 78712, and Baytown Chemical Plant, ExxonMobil Chemical Company, 5000 Bayway Drive, Baytown, Texas 77520

Industrial process monitoring tools require robust and efficient estimation techniques that maintain a high service factor by remaining online during abnormal operating conditions, such as during loss of measurements, changes in control status, or maintenance. Constraints incorporate additional process knowledge into estimation by bounding estimated disturbances within feasibility limits thereby providing robustness to faulty measurements or conditions that violate process models. Moving horizon estimation (MHE) and unscented Kalman filtering (UKF) are two estimation techniques that permit incorporation of constraints prior to evaluating the a priori estimate. This paper evaluates both constrained nonlinear estimators versus the extended Kalman filter (EKF) using industrial process data provided by ExxonMobil Chemical Company. Results provide short-term insight into the fouling process, and parameter estimates produced by UKF and MHE are shown to be more accurate than EKF.

1. Introduction

State and parameter estimation have demonstrated valuable application in the chemical process industries by enhancing process monitoring and control. Examples of industrial applications include offline and online process system identification, online monitoring and fault detection, parameter estimation for use in model predictive control, and process disturbance prediction. These estimation techniques may be Bayesian if the estimator represents the probability distribution with a collection of unique point estimates or deterministic if the distribution is characterized by its moments, for example, the mean and covariance. Techniques also vary in whether they retain past data as with batch estimation or propagate the distribution as with sequential estimation. This paper presents an investigation of several constrained deterministic sequential estimation techniques for monitoring fouling in an industrial chemical reactor at ExxonMobil Chemical Company's Baytown Chemical Plant.

Fouling directly affects the economics of the reactor operation. When fouling is removed, temperature control of the reactor is more accurate and provides more consistent reactor product qualities. In addition, scheduled cleanouts directly impact productivity by requiring the full product line upstream and downstream of the reactor to quit operation until the reactor is replaced. However, failure to clean the reactor prior to significant fouling accumulation will result in plugging of downstream lines and downtime greater than that required for a cleanout. Implementing a fouling monitor is critical to optimizing the schedule of cleanouts and gaining process knowledge of the fouling mechanism.

Traditional methods for estimating fouling assume that measurements are at steady-state or require local measurements. Alternative data reconciliation techniques, such as the Huber M-estimator, are based on linear regression; however, the fouling process has been shown to be nonlinear in recent works, and the linearity assumption will be an additional source of model mismatch. These issues have motivated recent work on developing fouling estimations that can use nonlinear physical dynamic models and utilize bulk measurements. Jonsson et al. proposes a method to model a heat exchanger based on conservation laws and estimates two dimensionless parameters for the heat transfer units for the hot and cold side tubes using the extended Kalman filter (EKF). Their work incorporates mass flow and inlet and outlet temperature measurements from a consecutive set of reliable, dynamic data.[1] Zavala et al. likewise develop a physical, dynamic model for estimating fouling of a multizone tubular low-density polyethylene reactor. The authors of that work justify using the moving horizon estimation (MHE) since it is capable of utilizing sophisticated dynamic models and handling bound constraints that prevent the estimated parameter from entering unreal regions.[2] In the present paper (unscented Kalman filtering) UKF is likewise capable of incorporating bound constraints, and the index-1 differential and algebraic equation (DAE) model can be simplified to ordinary differential equation (ODE) form for UKF and EKF.

Deterministic sequential estimation techniques have primarily evolved from the recursive least-squares solution used to derive the Kalman filter. The KF produces the optimal estimate given a linear, time-invariant, unconstrained system with Gaussian noise and propagates noise with the mean and covariance. The EKF refers to a class of estimation techniques that linearize nonlinear state and observation equations about the current operating state and use the optimal Kalman gain for updating the nominal trajectory. While the EKF has been commonly used in practice for unconstrained systems, key limitations of EKF are the inability to incorporate physical constraints accurately and inaccuracies in the Jacobian linearization causing estimate divergence.[3] These challenges have motivated alternative estimation techniques that retain the nonlinear system and incorporate physical constraints.

Two estimation techniques capable of accurately representing nonlinear dynamics without linearization and incorporating estimate constraints are UKF[4] and MHE.[5] An additional benefit of MHE is the capability of directly handling DAE models without simplification to ODE. Both techniques are sequential and deterministic. However, UKF represents system nonlinearity in a probabilistic manner by sampling the distribution initially at sigma points. Within UKF, the sigma points are transformed through the state-update and measurement-update equations. The a priori estimates and covariance matrices are calculated directly from the state sample and propagated using the KF equations.

* To whom correspondence should be addressed. Tel.: 678-575-9940. E-mail: bspivey@mail.utexas.edu.

† The University of Texas at Austin.

‡ ExxonMobil Chemical Company.

10.1021/ie9018116 © 2010 American Chemical Society
Published on Web 05/19/2010

UKF can also incorporate state or parameter equality and inequality constraints within the Kalman update and with sigma point clipping, respectively.[6,7] Sigma point clipping is unique from EKF clipping constraints, as it is performed a priori thereby constraining the distribution and resulting in modified covariance matrices and Kalman gains.

MHE is unique from Kalman filter techniques, as the joint probability distribution of prior state estimates is maximized rather than the a posteriori estimate distribution. In this sense, MHE is similar to a full information estimation, as a batch of prior states or parameters is estimated at each time step. However, the computational burden is reduced within MHE by truncating past data to a specified number of previous time periods. The horizon is shifted by a single time step at each iteration and provides the initial state for solving the optimization problem at the next time. MHE is formulated as a quadratic programming problem and is commonly solved using sequential quadratic programming (SQP). Inequality and equality constraints are incorporated directly into the optimization problem to be solved simultaneously with model equations. Liebman and Edgar proposed using nonlinear programming to perform data reconciliation with chemical systems characterized by highly nonlinear regions.[8] The formulation of MHE as a minimization of the sum of squared errors is proposed by Muske and Rawlings,[9] Michalska and Mayne,[10] and Robertson et al.[5] Sufficient conditions for stability of MHE formulation have been proven by Rao and Rawlings.[11] Zavala and Biegler demonstrated a fast MHE formulation based on expedited covariance information extraction to reduce computation time.[12] Other reports of MHE applications using online industrial chemical process measurements include monitoring diluent loss,[13] a feed blending application,[14] a gas-phase polymer reactor,[15] and a high pressure polymer reactor.[16]

In this paper, the performance of constrained UKF and MHE estimators are evaluated versus EKF for estimating industrial chemical reactor fouling using a nonlinear dynamic model. Constrained estimation is beneficial for most physical systems to prevent infeasible estimates, to satisfy conservation laws, and to improve the service factor of industrial process monitoring applications. From an operational perspective, robust monitors that recover automatically following abnormal conditions will perform at a higher service factor than monitors requiring manual reboot. The reasons for the lower service factor are listed as follows: the operator may require engineer assistance in returning the monitor online; the time lag between process recovery and monitor recovery will not be repeatable as it will vary by operator and time; and in particular, new monitors will likely not be a first priority for operators to return online following unplanned measurement losses or process excursions that cause bad estimate values. Thus consistent information following process recovery will be lost with manual involvement. The robust monitor will guarantee that important information following the event is captured, such as process performance with clean or new equipment.

Mangold et al. compared a square root UKF to a similar estimator termed *state estimation by online minimization* for estimating barium sulfate particle distributions. This approach of quasi-batch estimation differs from MHE, as the batch time intervals do not overlap and systems are unconstrained.[17] To the best of our knowledge, this paper is the first comparison of an inequality constrained unscented Kalman filter and moving horizon estimator. This work was performed in conjunction with the ExxonMobil Chemical Company at the Baytown Chemical Plant.

The paper is organized as follows: the derivation and algorithms for UKF and MHE are presented in section 2; section 3 presents results of the state and parameter estimation using UKF, MHE, and EKF; in section 4 we summarize conclusions and propose future work.

2. Preliminaries

2.1. Constrained UKF Algorithm. The unscented Kalman filter enables use of the Kalman update equations without linearizing the nonlinear state or observation equations, f and g, which are continuous in our application as follows:

$$\begin{aligned} \dot{x} &= f(x, u, w) \\ y &= g(x) + v \end{aligned} \tag{1}$$

in which x is the state vector, w and v are the state and observation noise, respectively, u is the state equation input vector, and y is the observation vector. Note that the state vector, x, may include constant model parameters that will be estimated.

The state vector is augmented as x_a to include the state vector, state noise, and observation noise, and the covariance matrix is augmented as P_{xa} in the same manner to include these terms.

$$x_{a,0} = \begin{bmatrix} x \\ w \\ v \end{bmatrix} = \begin{bmatrix} x \\ 0 \\ 0 \end{bmatrix} \tag{2}$$

$$P_{xa,0} = E[(x_a - \bar{x}_a)(x_a - \bar{x}_a)^T] = \begin{bmatrix} P_x & 0 & 0 \\ 0 & P_w & 0 \\ 0 & 0 & P_v \end{bmatrix}$$

in which $x_{a,0}$ and $P_{xa,0}$ are the initialized augmented state vector and covariance matrix, respectively.

Initial sigma points, X_i^-, are generated at time t as shown in eq 1 using the estimated value of x_a at the previous time such that $\bar{x} = \hat{x}_a$ and $P_x = P_{xa}$. Any dimension of the sigma point vector, X_i^-, that violates an inequality constraint is replaced by the boundary value.[7] Figure 1 demonstrates a two-dimensional sigma point constrained within the hatched region by inequality constraints.

Time-Update Equations. Each sigma point is propagated by integrating the nonlinear state and observation equations to produce current time state and observation sigma points, X^+ and Y^+.

$$\begin{aligned} X_i^+ &= \int_{t-1}^{t} f(X_i^-, u)\, dt, \\ Y_i^+ &= g(X_i^+) \end{aligned} \tag{3}$$

The current sigma points X^+ are constrained in the same manner as the initial sigma points, as shown in Figure 1. These points are used to characterize the mean and covariance of the a priori state estimate as follows:

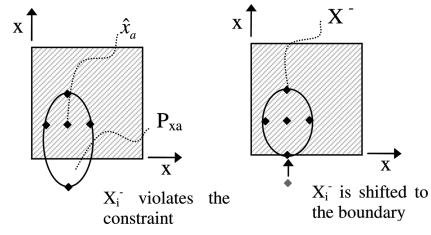

Figure 1. The initial covariance (left) exceeds constraints. After the constraint is applied, the covariance matrix and all sigma points satisfy constraints (right).

$$\begin{aligned}\bar{x}_a &= \sum_{i=1}^{p} w_{m,i} X_i^+ \\ \bar{y} &= \sum_{i=1}^{p} w_{m,i} Y_i^+ \\ \bar{P}_{xa} &= \sum_{i=1}^{p} w_{c,i}(X_i^+ - \bar{x}_a)\end{aligned} \tag{4}$$

in which the weights are generated in the same manner as in Wan:[18]

$$\begin{aligned}w_{m,0} &= \frac{\lambda}{L+\lambda} \\ w_{c,0} &= \frac{\lambda}{L+\lambda} + 1 - \alpha^2 + \beta \\ w_{m,i} &= w_{c,i} = \frac{1}{2(L+\lambda)}\end{aligned} \tag{5}$$

The observation covariance matrix, P_{yy}, and state-observation cross-covariance matrix, P_{xy}, are calculated to compute the optimal Kalman gain. Calculating the Kalman gain, K, using the sampling approach rather than linearization enables UKF to provide at least second-order accuracy with third and fourth-order accuracy possible for non-Gaussian distributions.

$$\begin{aligned}P_{yy} &= \sum_{i=1}^{p} (Y_i^+ - \bar{y})(Y_i^+ - \bar{y})^T \\ P_{xy} &= \sum_{i=1}^{p} (X_i^+ - \bar{x})(Y_i^+ - \bar{y})^T \\ K &= P_{xy} P_{yy}^{-1}\end{aligned} \tag{6}$$

Measurement-Update Equations. A posteriori updates to the state and covariance are performed using the Kalman gain update equations as follows:

$$\begin{aligned}\hat{x}_a &= \bar{x}_a + K(y_{obs} - \bar{y}) \\ P_{xa} &= P_{xa} - K P_{yy} K^T\end{aligned} \tag{7}$$

in which y_{obs} is the observation vector.

Linear equality constraints can be enforced in several manners, as derived by Simon.[6] The projection approach includes the equality constraints into derivation of the Kalman filter. Using a minimum variance derivation, the maximum probability estimate is provided with the following correction to the a posteriori state estimate:

$$\tilde{x}_a = \hat{x}_a - P_{xa} D^T (D P_{xa} D^T)(D\hat{x}_a - d) \tag{8}$$

where $\tilde{x}_a$ is the a posteriori state estimate corrected with constraints, D is a matrix containing the algebraic relationship between states in constraint equations, and d is a vector containing the constraint constants.

2.3. Moving Horizon Estimation. MHE is an approximation to the full information state estimator (FIE) whereby a mathematical program is solved over a horizon limited to the previous N measurements as follows:

$$\min_{x_{T-N}, w_k} \Phi_T(x_{T-N}, w_k, v_k)$$

$$\Phi_T(x_{T-N}, w_k, v_k) = \sum_{k=T-N}^{T-1} \left(\left\| v_k \right\|_{R^{-1}}^2 + \left\| w_k \right\|_{Q^{-1}}^2 \right) + Z_{T-N}(x_{T-N})$$

subject to

$$\begin{aligned}0 &= f(\dot{x}, x, u) \\ 0 &= g(y, x, u, v) \\ h(x, u, w) &\le 0\end{aligned} \tag{9}$$

in which w_k and v_k are the state and observation disturbances at time k, Q and R are the estimated state and observation noise covariance matrices which may be used as tuning parameters, and Z_{T-N} is the arrival cost which incorporates estimate knowledge prior to the horizon. For nonlinear models, the arrival cost will necessarily be an approximate estimate.[19] Methods for handling the arrival cost include using EKF, UKF, or discarding the arrival cost altogether by considering it as a constant function.

MHE problem is solved using a sparse nonlinear programming (NLP) solver, suitable for large-scale systems of industrial process monitoring. The specific MHE software application and NLP solver used are proprietary and cannot be disclosed; however, algorithm used in this work is characterized by the following: inequality constraints on states and parameters; the arrival cost term is neglected; state and observation disturbances do not include white noise in the model; an optimization cost on estimated state moves.

These modifications have been included to enhance estimator stability and reduce the computational burden. In particular, past experience has shown that the increased computational burden of computing the arrival cost has not justified by potential improvements in accuracy or tuning of the moving horizon estimation algorithm; therefore, the arrival cost has been neglected within the algorithm used for this study. The modified nonlinear programming problem is presented as follows:

$$\min_{d} \Phi$$

$$\Phi = \sum_{k=T-N}^{T-1} \left(\left\| v_k \right\|_{R^{-1}}^2 + \left\| d_k \right\|_{W^{-1}}^2 \right)$$

subject to

$$\begin{aligned}0 &= f(\dot{x}, x, d, u) \\ 0 &= g(y, x, d, u, v) \\ h(x, d, u, w) &\le 0\end{aligned} \tag{10}$$

in which d_k is equal to the delta in estimated states from the previous solution to current estimate, h contains the algebraic state constraints, and v represents the observation residual without additive noise. MHE constraints on model disturbances constrain the a posteriori probability distribution function and increase the probability at valid state values.[19]

2.4. Comparison. In the same manner as MHE, the Kalman filter is derived from the least-squares objective function shown as follows:

$$\Phi = \sum \left\| v_k \right\|_{R^{-1}}^2 = \sum_i (Y_i - \bar{y}) R^{-1} (Y_i - \bar{y})^T \tag{11}$$

A similar feature of all Kalman filtering techniques is that they provide a linear update that can be derived from eq 11 using the maximum likelihood estimate. UKF employs sigma-point sampling to estimate the covariance matrices within the linear update. MHE minimizes the objective function by posing the model equations, additional constraints, and objective

function as a mathematical programming problem. Additional differences between UKF and MHE include the sequential nature of KF versus the batch nature of MHE, nonlinearity approximation, constraint handling, and system model formulation.

A framework for comparing MHE and UKF accuracy is made by considering batch least-squares estimation (BLSE) versus KF. BLSE is derived using the same objective function as KF but is iterative and incorporates all past observations into the a posteriori state estimate calculation. All results from the first iteration of BLSE, including the estimate and residuals, are equal to the final results of the Kalman filter over the same horizon of data. However, since BLSE is iterative, the accuracy of BLSE is naturally greater than or equal to the accuracy of KF.[20] MHE is similar to BLSE in minimizing the least-squares error of the residual in an iterative manner, whereas UKF is a sequential estimator. Both MHE SQP solver and UKF algorithms employ second-order estimates at each iteration; however, the SQP solver continues to iterate until the convergence tolerance is satisfied. This is a robust means of guaranteeing local optimality without tuning.

Incorporating inequality constraints directly into the Kalman filter derivation requires an active set approach and necessitates the use of mathematical programming solvers.[6] Hence, the a posteriori state estimate cannot be constrained via inequalities using the traditional UKF. As shown previously, the a priori state estimate can be constrained using sigma-point constraints. With MHE, the final state estimates are constrained within the mathematical programming problem. UKF and MHE constraint methods, as used in this paper, also constrain the state estimate probability distribution. Application of state constraints requires consideration of how the state constraints may create causality between the state equation disturbances and states as demonstrated by Rao and Rawlings.[19]

MHE is an ideal estimator for DAE models since the model may be retained in DAE form without converting to ODE form. The model is incorporated directly into the mathematical programming problem as a constraint. For black-box input−output models, which may contain logic statements and loops, UKF is an ideal choice since only the model output is needed for estimation.

For the purposes of comparison in this paper, the DAE model of the industrial reactor is index-1 and may be algebraically rearranged to ODE form for UKF and EKF comparisons. MHE model equations in eq 10 are posed in an open equation form that allows for the fewest restrictions on model structure and facilitates solving DAE models. At the solution, the NLP solver closes the residuals of the open form DAEs. Kalman filter techniques require a model in semiexplicit ODE form as shown in eq 1. However, for many first principles models the conversion from DAE to ODE form is not practical or impossible. For instance, chemical process models often employ the quasi-steady-state (QSS) assumption to reduce model stiffness.[21]

3. Industrial Fouling Monitoring Application

Constrained unscented Kalman filtering and moving horizon estimation have been applied to predict process fouling of an industrial stirred tank reactor at ExxonMobil Chemical Company. This fouling model presents several challenges appropriate for our evaluation of constrained nonlinear estimation: nonlinear dynamics in the state and measurement equations; real process data including abnormal operation events; inherent process-model mismatch; and transport delays causing measurements to be offset in time.

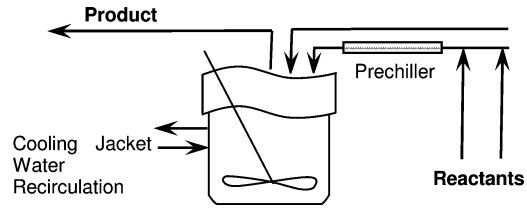

Figure 2. A simplified diagram of the exothermic CSTR.

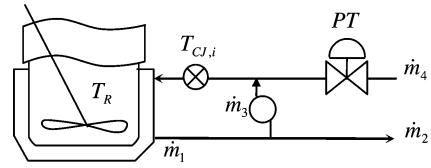

Figure 3. Jacketed cooling water system for the CSTR.

3.1. Energy and Mass Conservation Model. Process Overview. Reactants are mixed in upstream lines and fed to a continuously stirred tank reactor (CSTR) for chemical activation before entering into the main process lines. Mixing in upstream lines and within the CSTR produce exothermic reactions, and the CSTR temperature must be actively controlled via an external jacketed cooling water system; the control system consists of a PID cascade controller on the cooling water feed valve. It is important to note that the estimator can utilize the dynamic closed-loop measurement data to provide an accurate measure of fouling. As mentioned in the introduction, traditional fouling estimators require steady-state data and occasional halting of process operation. A diagram of the chemical process equipment is shown in Figure 2.

Fouling in this application and most heat exchangers is well-known to insulate the hot process line from dedicated sources of cooling necessary to maintain process operating temperatures. As a result fouling degrades the cooling effectiveness of the heat exchanger system. In this particular chemical process, fouling is a mixture of reactants that coalesces to the side of the reactor thereby insulating the reactor and decreasing the overall wall heat transfer coefficient. Fouling of the reactor walls causes loss of temperature control and increases the risk of downstream plugging due to fouling particle release.

The available process knowledge indicates that as the cooling jacket wall decreases in temperature, the rate of wall fouling increases; hence, the fouling process is nonlinear. The fouling estimator has assisted in determining an improved schedule for cleanout and replacement. Additionally, the online monitoring application identifies operating conditions that lead to higher fouling rates.

Process Model. The jacketed cooling water system, shown in Figure 3, has been chosen as the estimation model rather than the chemical process, as the cooling water system presents fewer unknown physical parameters.

A gray-box model comprised of a DAE system is used to approximate the cooling system performance with a combination of first principles mass and energy balances and an empirical valve coefficient model as follows:

Internal cooling jacket energy balance:

$$\rho V c_p \frac{dT_{CJ,o}}{dt} = \dot{m}_1 c_p (T_{CJ,i} - T_{CJ,o}) + UA_{CJ}(T_R - T_{CJ,o}) + h_{amb}(T_{amb} - T_{CJ,o}) \quad (12)$$

External piping energy balance:

$$\dot{m}_1 c_p (T_{CJ,o} - T_{CJ,i}) = \dot{m}_2 c_p T_{CJ,o} - \dot{m}_4 c_p T_{WRS} - W_p \quad (13)$$

Mass balances:

$$\dot{m}_1 = \dot{m}_{4,lag} + \dot{m}_3 \quad (14)$$

$$\dot{m}_2 = \dot{m}_1 - \dot{m}_3 \quad (15)$$

Control valve mass flow:

$$\dot{m}_4 = \rho k_v \sqrt{\frac{p_s - p_a}{\gamma_{H_2O}}} \quad (16)$$

Experimental valve coefficient:

$$k_v = \alpha e^{(\beta PT)} + \delta \quad (17)$$

Measurement time delay:

$$\tau \frac{d\dot{m}_{4,lag}}{dt} = -\dot{m}_{4,lag} + \dot{m}_4 \quad (18)$$

The external piping energy balance, eq 13, is modeled as steady-state as is typical with insulated piping for incompressible fluids over relatively short distances.

3.2. Estimation. The fouling model is created to estimate the overall heat transfer coefficient, UA_{CJ}, as an indicator of fouling thickness. The cooling jacket inlet temperature, $T_{CJ,i}$, is the measured output. Three additional measured variables are incorporated as model inputs: the lumped CSTR temperature, T_R, the ambient temperature, T_{amb}, and the control valve percent travel, PT. As the measured inlet temperature, the $T_{CJ,i}$, response is consistently delayed from the valve action by approximately 2 min, we include a first-order time delay on the inlet mass flow, eq 18. This dynamic effect could also be handled by incorporating a delayed mass flow measurement within MHE algorithm; a first-order time delay equation is more feasible for the algorithm used in this paper.

3.3. Results. Results of this study demonstrate a successful application of MHE and UKF for industrial process monitoring in the presence of noisy data during normal operation and faulty measurements during a maintenance operation. Whereas an unconstrained MHE or UKF estimator will often fail to solve when faulty measurements cause estimates to enter infeasible regions, the incorporation of estimated state or parameter constraints enables the estimation routine to remain online and recover automatically once repaired. In industrial settings, monitoring tools that fail regularly during either planned or unplanned process faults will naturally experience decreased service time and lose favor with operators.

In the present application, faulty measurements occur during maintenance when at least one of the required measurements for process monitoring is removed and the operational nature of the process is changed sufficiently to invalidate the normal operating model. The authors also considered modelling the process structure during the abnormal operating condition to develop a more complex fault-detection scheme; however, the available measurements during this period were not sufficient to produce an accurate model. The following results are produced using process monitoring based on parameter estimation.

The previously shown process model is employed within an online MHE-based process monitoring tool loaded on the distributed control system, and the estimated heat transfer coefficient shown for MHE has been retrieved from historical data. Results for UKF and EKF have been produced via offline simulation in MATLAB. EKF has been included to provide a baseline comparison of a technique that requires model linearization versus techniques that estimate model nonlinearity, MHE and UKF. The EKF algorithm is adapted from the extended sequential filter as shown by Tapley and is not modified to include constraints.[21]

Table 1. Constraints on the Estimated Overall Heat Transfer Coefficient (UA_{CJ})

	lower bound	upper bound
MHE	30	10000
UKF	30	1000

Inequality parameter constraints are applied to UA_{CJ}, as shown in Table 1. The constraints proved necessary to provide high service factors for online monitoring. Without the parameter constraints, both algorithms fail to continue solving in the presence of abnormal operating conditions during which the model is invalid and measurements are faulty.

UKF algorithm required tuning beyond that required by MHE to ensure operation without failure. The estimated heat transfer upper bound was reduced from MHE bound of 10000. MHE bound was not altered for these results since MHE results are provided from historical data. In addition, UKF required careful tuning of the covariance matrix coefficients to achieve a robust solution.

The measurement period used for the estimated heat transfer coefficient, shown in Figure 4, includes an abnormal event to illustrate how the estimator remains online with bad data. The said event is a reactor cleanout during which the jacketed cooling system control is shutdown and model assumptions are expected to be violated. A plot without the constraints would simply show the estimated parameter diverging and then stopping at the time at which the estimator solution fails.

As shown in Figure 4, the overall heat transfer coefficient increases over a factor of 2 following the reactor cleanout. The results clearly indicate fouling removal during the reactor cleanout operation on August 28 as it has been explained that fouling decreases the heat transfer coefficient in this application. Observing the immediate increase of heat transfer coefficient following the cleanout is critical to validate proper operation of UKF and MHE based on process knowledge. In addition, these plots provide insight into the short-term fouling process. The results demonstrate that the heat transfer rate for a clean reactor is several times greater than a fouled reactor. The reactor fouls more quickly during the first day immediately following the cleanout; however, the rate of fouling slows to a similar rate as shown prior to the cleanout.

The upper and lower bound constraints are active during the reactor cleanout for the parameter estimated via MHE and UKF. Preliminary tests have shown that without these constraints the estimated heat transfer coefficient will exceed the constraints and ultimately cause the estimator to fail. Had the estimator been online without constraints, an operator would be responsible for manually restarting the estimator follow every such event, and valuable estimates of the heat transfer coefficient immediately following cleanout are likely to be lost. In addition, unplanned process excursions, such as loss of measurement data, can cause an unconstrained estimator to fail as explained if constraints are not included. A key intangible element of any online process monitoring tool is gaining trust of operations to utilize the data. Were the fouling monitor to fail on a regular basis and require significant manual interaction, operators would likely choose not to utilize or trust monitoring results. Ultimately, failure to remain online would result in lost economic opportunity. The benefit of constraints is apparent for this application.

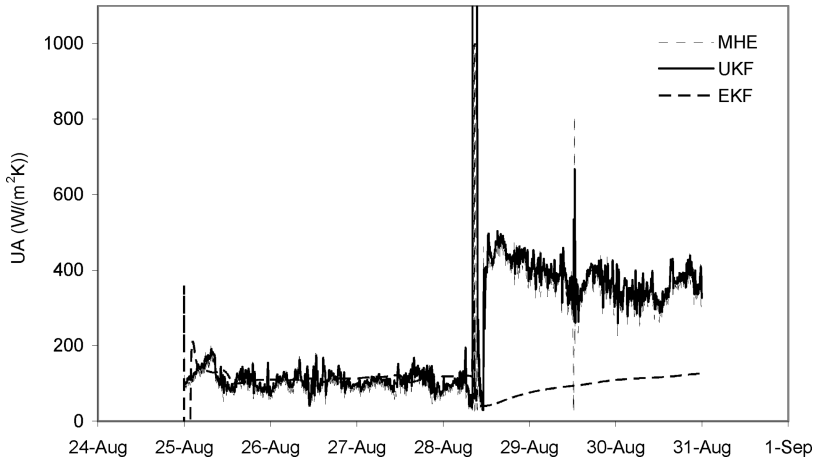

Figure 4. Estimated overall heat transfer coefficient for MHE, UKF, and EKF.

Both nonlinear estimators, MHF and UKF, provide similar estimation performance. The linear estimation provided by EKF approximates the nonlinear estimator results prior to the cleanout event but fails to recover to an accurate value following the cleanout. Calculating the estimation residuals is used to verify that UKF and MHE results are more accurate than the EKF results. Process knowledge indicates that the heat transfer coefficient should increase after fouling removal; however, the estimated parameter alone does not quantitatively distinguish which is the accurate set of results. Thus the estimation residuals are a critical indicator of estimator performance by quantifying the difference between the measured output and output that is calculated from the model. The magnitude of residuals is also an important indicator for how well the estimator satisfies the conservation equations at each time as the calculated output is the reactor inlet temperature. Estimation residuals, dy_i, and the mean squared error, MSE, are calculated according to

$$dy_i = y_{\text{obs}} - y_{\text{model}}$$
$$\text{MSE} = \frac{1}{m}\sum_{i=1}^{m} dy_i^2 \tag{20}$$

Plots of the estimation residuals in Figure 5 indicate clearly that EKF has larger residuals than MHE or UKF following the reactor cleanout; note that the scale for the EKF plot is increased.

These results likewise agree with process knowledge and indicate that MHE and UKF provide accurate estimates. Overall, EKF is less accurate than UKF before and after cleanout. The decreased accuracy before the cleanout also explains why the EKF estimate is smoother than the nonlinear estimates—the EKF is failing to close the residual during this time.

The use of a linear Jacobian estimate of model nonlinearity explains the reduced accuracy with EKF. Linear approximations are necessary to update the state transition matrix and information matrix. MHE residuals are somewhat higher than UKF residuals, but MHE is noticeably more accurate than EKF. For this application, operations will be monitoring the estimated heat transfer coefficient over a period of weeks, and MHE estimate is satisfactory. As seen in Figure 4, MHE estimate is characterized by less noise than UKF estimate. The mean squared errors (MSE) are shown in Table 2.

The MSE from the full dataset includes data that are misleading since it also considers results during the reactor cleanout when the model is not expected to be valid; UKF produces worse residuals during the abnormal events, thereby penalizing the MSE. A box plot may be used to identify residuals; however, for this study, using a box plot disadvantaged the EKF by identifying more outliers for UKF and MHE. A more accurate approach for identifying outliers for this case was to remove the same number of data points for each method. Outliers were identified as the one-half percent of the data points with the highest squared residual for each method. When outliers during the transition period are removed, the MSE coincides with the residual plots, indicating that UKF has a lower residual for a majority of the data.

While UKF and MHE both provide acceptable estimates, the smaller residuals produced by UKF may be explained by the difference in estimation problem formulation. UKF calculates an update for the two differential states, $\dot{m}_{4,\text{lag}}$ and $T_{\text{CJ,o}}$, in addition to the heat transfer coefficient. In particular, $T_{\text{CJ,o}}$, is corrected near the same magnitude as the residual at each iteration within UKF. In an effort to compare MHE to UKF more fairly, estimated noise variables for the two differential states were included in MHE model, and the state noise was constrained as $|v_1| \leq 1$ and $|v_2| \leq 3$ for $\dot{m}_{4,\text{lag}}$ and $T_{\text{CJ,o}}$, respectively. However, this approach provided too many degrees of freedom and led to unrealistic estimates for the heat transfer coefficient. The algorithm adjusted the noise variables to compensate for model-mismatch rather than the heat transfer coefficient.

As necessary for online application, all techniques provide updates more quickly than real-time measurements, which arrive in one minute intervals, as shown in Table 3.

This comparison illustrates that the computational burden of MHE can be competitive to UKF. MHE is performed with proprietary modeling and control software written in Fortran and C++. UKF and EKF algorithms were formulated in MATLAB. All simulations for computational comparison were performed on a 3.60 GHz Intel Xeon-processor PC.

In summary, the results indicate that MHE and UKF provide accurate estimates of the reactor fouling and remain online despite loss of measurement data and process changes that invalidate the basic operating model—temperature probes are removed and a cooling system valve is set to prevent normal operation during maintenance. The estimator has demonstrated robust operation through the planned maintenance operation. Robust operation makes an economic benefit of the estimator possible. Economic benefit is realized by preventing an unnecessary cleanout per year which would otherwise be performed in absence of a fouling estimate. Preventing one cleanout is sufficient incentive to justify the time required to develop the fouling process monitor. The cleanout operation is only one

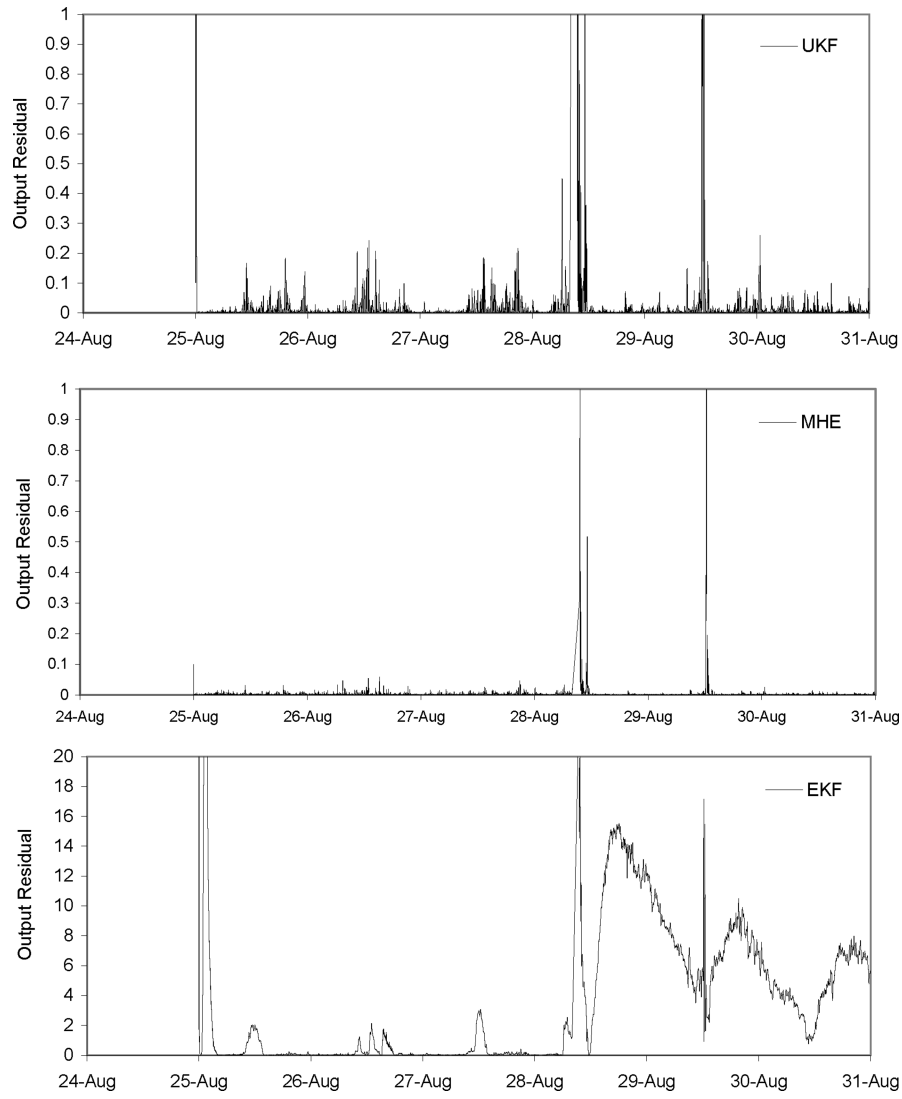

Figure 5. Residual plots for MHE, UKF, and EKF.

Table 2. Mean Squared Error of the Output Calculation

	Mean Squared Error	
	full data set	full data set excluding transition period
MHE	0.0296	0.0148
UKF	2.4925	0.0021
EKF	3.4838	3.2295

Table 3. Average Computation Time between Each A Posteriori Estimate

	CPU time(s)
MHE	0.3639
UKF	0.2218
EKF	0.0515

example of a planned or unplanned process fault. Insight into the short-term fouling process is provided, and the online monitoring tool is currently under observation for long-term estimator performance, and process knowledge gained from long-term performance remains for future work.

4. Conclusions

Adding constraints to estimators introduces additional process knowledge into the estimation routine. Estimated state or parameter distributions are often bounded by feasibility limits outside of which the estimator is much more likely to fail. Constraints enable the propagated distribution to incorporate knowledge of the feasible operating region. A method of introducing sigma-point constraints in UKF was evaluated versus MHF to estimate disturbances on a nonlinear gray-box model. The study also demonstrates the estimation challenge presented by the nonlinear process model by comparing UKF and MHE to extended Kalman filtering. All evaluations were performed using industrial process data.

A nonlinear model based on conservation laws was developed to estimate fouling thickness within an exothermic continuously stirred-tank reactor at the Baytown Chemical Plant within ExxonMobil Chemical Company. The heat transfer coefficient between the reactor and jacketed cooling system was estimated as an indicator of fouling thickness.

The evaluation of constrained nonlinear estimation techniques indicates that both constrained UKF and MHE produce heat transfer coefficient estimates that agree with generic process knowledge. The constraints are critical in this application to ensure the estimators continue solving online during atypical plant operation. EKF results fail to converge following the maintenance operation, which demonstrates inaccuracy in the Jacobian approximation to the nonlinear model. For this comparison, MHE and constrained UKF were both competitive in estimation accuracy and computational requirements for a

nonlinear industrial estimation problem with faulty data. In general, MHE is a more accurate algorithm as discussed in the comparison of batch and sequential estimation and is capable of handling problems in implicit DAE form; UKF may be preferred when legacy black-box models must be used since the internal logic may prevent using the model directly as a set of NLP constraint equations.

As future work, the authors propose a comparison between UKF and MHE to solve a large-scale constrained estimation problem using comparable computing architecture. In addition, future work for this specific application includes translating the estimated heat transfer coefficient directly into a fouling thickness measure and monitoring long-term performance to gain additional fouling process knowledge. The present work was beneficial to discuss capabilities and limitations of MHE and UKF with similar criteria and compare these techniques with industrial data.

Acknowledgment

The authors thank Tyler Soderstrom for helpful review comments and ExxonMobil Chemical Company for hosting and supporting Benjamin Spivey during this project.

Literature Cited

(1) Jonsson, G. R.; Lalot, S.; Palsson, O. P.; Desmet, B. Use of extended Kalman filtering in detecting fouling in heat exchangers. *Int. J. Heat Mass Transfer* **2007**, *50*, 2643.

(2) Zavala, V. M.; Biegler, L. T. Optimization-based strategies for the operation of low-density polyethylene tubular reactors: Moving horizon estimation. *Comput. Chem. Eng.* **2009**, *33*, 379.

(3) Haseltine, E. L.; Rawlings, J. B. Critical evaluation of extended Kalman filtering and moving-horizon estimation. *Ind. Eng. Chem. Res.* **2005**, *44*, 2451.

(4) Julier, S. J.; Uhlmann, J. K. Unscented Filtering and Nonlinear Estimation. *Proc. IEEE* **2004**, *92*, 401.

(5) Robertson, D. G.; Lee, J. H.; Rawlings, J. B. A moving-horizon based approach for least squares estimation. *AIChE J.* **1996**, *42*, 2209.

(6) Simon, D. *Optimal State Estimation: Kalman, H Infinity and Nonlinear Approaches*; Wiley-Interscience: Hoboken, NJ, 2006.

(7) Kandepu, R.; Foss, B.; Imsland, L. Applying the unscented Kalman filter for nonlinear state estimation. *J. Process Control* **2008**, *8*, 753.

(8) Liebman, M. J.; Edgar, T. F.; Lasdon, L. S. Efficient data reconciliation and estimation for dynamic processes using nonlinear programming techniques. *Comput. Chem. Eng.* **1992**, *16*, 963.

(9) Muske, K. R.; Rawlings, J. B. *Receding Horizon Recursive State Estimation*; Proceedings of the American Control Conference, San Francisco, CA, 1993.

(10) Michalska, H.; Mayne, D. Q. Moving horizon observers and observer-based control. *IEEE Trans. Automat. Control* **1995**, *40*, 995.

(11) Rao, C. V.; Rawlings, J. B. *International Symposium on Nonlinear Model Predictive Control*; Ascona, Switzerland, 1998.

(12) Zavala, V. M.; Laird, C. D.; Biegler, L. T. A fast moving horizon estimation algorithm based on nonlinear programming sensitivity. *J. Process Control* **2008**, *18*, 876.

(13) Soderstrom, T. A.; Edgar, T. F.; Russo, L. P.; Young, R. E. Industrial application of a large-scale dynamic data reconciliation strategy. *Ind. Eng. Chem. Res.* **2000**, *39*, 1683.

(14) Rajamani, M. R.; Rawlings, J. B.; Soderstrom, T. A. Application of a new data-based covariance estimation technique to a nonlinear industrial blending drum. Submitted for publication.

(15) Hedengren, J.; Allsford, K.; Ramlal, J. *Moving Horizon Estimation and Control for an Industrial Gas Phase Polymerization Reactor*; Proceedings of the American Control Conference, New York, NY, July, 2007.

(16) Zavala, V. M.; Biegler, L. T. Optimization-based strategies for the operation of low-density polyethylene tubular reactors: Nonlinear model predictive control. *Comput. Chem. Eng.* **2009**, *33*, 1735.

(17) Mangold, M.; Buck, A.; Schenkendorf, R.; Steyer, C.; Voigt, A.; Sundmacher, K. Two state estimators for the barium sulfate precipitation in a semi-batch reactor. *Chem. Eng. Sci.* **2009**, *64*, 646.

(18) Wan, E. A.; van der Merwe, R. The Unscented Kalman Filter. *Kalman Filtering and Neural Networks*; Haykin, S., Ed.; Wiley: New York, 2001.

(19) Rao, C. V.; Rawlings, J. B. Constrained process monitoring: Moving-horizon approach. *AIChE J.* **2002**, *48*, 97.

(20) Tapley, B. D. *Statistical Orbit Determination*; Elsevier, Academic Press: Boston, MA, 2004.

(21) Kumar. A.; Daoutidis, P. *Control of Nonlinear Differential Algebraic Equation Systems*; CRC Press: Boca Raton, FL, 1999.

Received for review November 15, 2009
Revised manuscript received January 22, 2010
Accepted April 26, 2010

IE9018116